



# Observational evidence of a long-term increase in precipitation due to urbanization effects and its implications for sustainable urban living



K.M. Wai <sup>a,\*</sup>, X.M. Wang <sup>b,\*</sup>, T.H. Lin <sup>c</sup>, M.S. Wong <sup>d</sup>, S.K. Zeng <sup>e</sup>, N. He <sup>f</sup>, E. Ng <sup>a,f,g</sup>, K. Lau <sup>g</sup>, D.H. Wang <sup>b</sup>

<sup>a</sup> Institute of Future Cities, Chinese University of Hong Kong, Hong Kong Special Administrative Region

<sup>b</sup> School of Atmospheric Sciences, Sun Yat-sen University, Guangzhou, China

<sup>c</sup> Center for Space and Remote Sensing Research, National Central University, Taiwan

<sup>d</sup> Department of Land Surveying and Geo-informatics, Hong Kong Polytechnic University, Hong Kong Special Administrative Region

<sup>e</sup> Graduate Institute of Space Science, National Central University, Taiwan

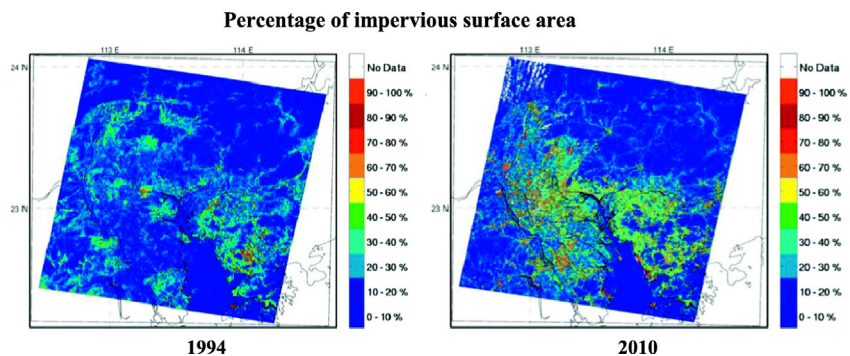
<sup>f</sup> Institute of Environment, Energy and Sustainability, Chinese University of Hong Kong, Hong Kong Special Administrative Region

<sup>g</sup> School of Architecture, Chinese University of Hong Kong, Hong Kong Special Administrative Region

## HIGHLIGHTS

- Analysed a ten-year precipitation dataset for a megacity and nearby stations
- Remote sensing techniques revealed rapid urbanization at the megacity.
- Significant increasing trend of precipitation existed only at the megacity station.
- Urbanization-induced increase is higher than that from the future climate change.
- Findings have implication to coastal defenses, disease spread and heat stress.

## GRAPHICAL ABSTRACT



## ARTICLE INFO

### Article history:

Received 12 December 2016

Received in revised form 27 March 2017

Accepted 2 May 2017

Available online xxx

Editor: Wei Ouyang

### Keywords:

Urbanization effects

Remote sensing

Long-term precipitation trend

WRF model

Climate change adaptation

Sustainable urban development

## ABSTRACT

Although projected precipitation increases in East Asia due to future climate change have aroused concern, less attention has been paid by the scientific community and public to the potential long-term increase in precipitation due to rapid urbanization. A ten-year precipitation dataset was analysed for both a rapidly urbanized megacity and nearby suburban/rural stations in southern China. Rapid urbanization in the megacity was evident from satellite observations. A statistically significant, long-term, increasing trend of precipitation existed only at the megacity station (45.6 mm per decade) and not at the other stations. The increase was attributed to thermal and dynamical modifications of the tropospheric boundary layer related to urbanization, which was confirmed by the results of our WRF-SLUCM simulations. The results also suggested that a long-term regional increase in precipitation, caused by greenhouse gas-induced climate change, for instance, was not evident within the study period. The urbanization-induced increase was found to be higher than the precipitation increase (18.3 mm per decade) expected from future climate change. The direct climate impacts due to rapid urbanization is highlighted with strong implications for urban sustainable development and the planning of effective adaptation strategies for issues such as coastal defenses, mosquito-borne disease spread and heat stress mortality.

© 2017 Elsevier B.V. All rights reserved.

\* Corresponding authors.

E-mail addresses: [bhkmwai@cityu.edu.hk](mailto:bhkmwai@cityu.edu.hk) (K.M. Wai), [eeswxm@mail.sysu.edu.cn](mailto:eeswxm@mail.sysu.edu.cn) (X.M. Wang).

<sup>1</sup> Current address: Environment and Climate Institute, Jinan University, Guangzhou, China.

## 1. Introduction

A median increase of precipitation of 9% in East Asia by the end of the 21st century is projected under the A1B scenario due to greenhouse gas-induced climate change (IPCC, 2007). Although this has aroused many discussions among the scientific community and the public, much less attention has been paid to changes in precipitation due to urbanization effects, and there has been little quantification of these effects. Globally, 54% of the population lived in urban areas in 2014, compared with 30% in 1950, and this population is projected to increase to 66% in 2050 (UN, 2015). Developing countries, such as those in Latin America and Africa, have undergone the process of rapid urban growth or are on the path towards it. A better understanding of the urbanization effects on the environment is required (van Ginkel, 2008). Urbanization replaces forests with buildings and roads and reduces the evaporation (and thus cooling) at the surface. Tall buildings reduce the ventilation rate and trap the heat within urban areas (Arnfield, 2003). These factors, as well as anthropogenic heating (Quah and Roth, 2012), cause urban heat island (UHI) effects in many mega-cities in the world. In China, land use/cover change and human activities were attributed to be the primary reason for the rising temperatures in Jiangsu Province (Huang et al., 2015). Since the 1970s, the enhancement of precipitation intensity has been linked to urbanization effects (METROMEX, 1974; Changnon, 1979). City (i) acts as the warm center to increase unstable air masses and (ii) increases the surface roughness to enhance surface convergence, which both mechanisms enhance the convection over and downwind of the city center (Hjelmfelt, 1982; Lin et al., 2008a). By analysis of six precipitation events, Bornstein and Lin (2000) showed that the UHI induced a convergence zone that initiated convective activities over and immediately downwind of Atlanta, Georgia, U.S.A. The findings were further supported by a study based on 5-year data on land-use, radar reflectivity, surface meteorological data and upper-air soundings (Dixon and Mote, 2003). The impacts on strong vertical convection were also reflected by lightning activities. Naccarato et al. (2003) reported an enhancement of 60–100% in the cloud-to-ground lightning flash density over Brazilian urban areas compared to their surroundings. Numerical model simulations (Hjelmfelt, 1982; Lin et al., 2008a; Zhong and Yang, 2015) are consistent with the anomalies found from observational studies. For example, sensitivity tests of the MM5 meso-scale model suggested that UHI perturbed thermal and dynamic processes at the atmospheric boundary layer and affected the location of precipitation over the western plain of Taiwan. Precipitation over the upwind area was also enhanced (Lin et al., 2008a) by the increasing size of the urban area. However, the above-mentioned studies mainly focused on short-term events.

The Pearl River Delta (PRD) is one of the rapidly developing areas in southern China. Urban area in the PRD was expanded from 0.5% to 12.9% from 1993 to 2004. Guangzhou, located in the PRD, is one of the largest megacities in China, along with Beijing and Shanghai, and has a population of approximately 25 M. The relationships between UHIs and land-use/land-cover changes in the PRD have been studied (Chen et al., 2006). They reported the percent of built-up area increased from 6.09% in 1990 to 13.08% in 2000, while the percent of cropland decreased from 42.23% to 21.48% for the same time span. Based on our simulations, precipitation increased 15% over urban and leeward areas in summer due to the urbanization of the Yangtze River Delta in eastern China (Zhang et al., 2010). In this study we attempted to provide, for the first time, observational evidence of long-term urbanization-induced enhancement of precipitation (UIEP). We first compared satellite products of surface temperatures between 1994 and 2010 to provide support for the existence of a UHI and urbanization over the Guangzhou megacity. Then, a 10-year daily precipitation dataset (1997–2006, covering a period of high urbanization rate in the Guangzhou megacity) of rain gauge measurements in and near the PRD was analysed to study the long-term urbanization effects on precipitation. The Weather Research and Forecasting (WRF) model, detailed later, was used to perform

numerical experiments to confirm the UIEP by simulations of typical precipitation events in summer. Finally, because the effects could become more significant in the future (Pielke et al., 2007), implications of the effects on sustainable urban planning were discussed.

## 2. Data and methodology

### 2.1. Satellite products

The large spatial coverage of satellite images makes them advantageous for detecting UHIs, which are city-scale phenomena. Land surface temperature ( $T_s$ ) derived from the satellite images has been used in many urbanization and UHI studies (Balling and Brazel, 1988; Dousset and Gourmelon, 2003; Nichol et al., 2009). Two Landsat images were acquired at 10:30 am (local time) on October 24, 1994 and October 28, 2010. The land surface temperature products at 30 m resolution were derived using the emissivity modulation method (Nichol, 2009) with correction of the emissivity of the original thermal channel using land use and land cover data.

The trend of urbanization in terms of the impervious surface area (ISA) was also evaluated to understand the land use change during the urban development. The impervious surface is the built environments, such as building, road and infrastructure, which can be an indicator of urbanization and related to urban heat island effects and regional energy balances (Sawaya, 2003). The ISA products currently presented were those being post-processed from the mentioned Landsat images. Following the study of Wu and Murray (2003), the ISA was calculated based on the result of land use classification (i.e., building, bare land, vegetation and water categories) within a specific area. The spatial distribution of ISA is generated from 5 by 5 pixels of window size all over the study area.

### 2.2. Surface precipitation measurements

The 10-year (1997–2006) surface daily precipitation measurements at various locations at and near the PRD were used to study if the urbanization had long-term effects on the precipitation amount. Rain-gauge measurements at Guangzhou (GZ; 23.1°N, 113.3°E), Fogang (FG; 23.8°N, 113.5°E), Lianpin (LP; 24.4°N, 114.5°E), Naxiong (NX; 24.9°N, 114.2°E) and Shaogua (SG; 24.7°N, 113.5°E) (Supplementary information Fig. S1) were used. The ISA is >80% for station GZ and are in the range of 0–30% for the rest of the stations. Guangzhou is a typical megacity in China, and the GZ urban station located near the Guangzhou metropolis is suitable for studying urbanization effects. Other stations near the Guangzhou metropolis are suburban or rural in nature and acted as controls to detect if any long-term, regional effects on precipitation occurred. To the south of the Guangzhou metropolis is the coastal line facing towards the South China Sea and the PRD (Fig. 1).

### 2.3. Trend analysis

The precipitation data at each selected station were first tested for trend significance by the well-known Mann-Kendall (M-K) test, which has been employed in trend investigations of precipitation and other environmental variables (Brunetti et al., 2001; Joshi and Pandey, 2011; Ziv et al., 2013). Details of the test have been described, for example, in Gilbert (1987) and the quoted references, and thus are not repeated here. Briefly, the M-K test computes the S- and Z-statistics to test a null hypothesis of no trend and an alternative hypothesis of the existence of a trend. We tested the null hypothesis at the 95% confidence level. Linear least-square regression was then used to quantify the trend magnitude when the trend at a station was determined to be statistically significant. Linear regression is a popular method for trend-magnitude studies (Liebmann et al., 2004; Groisman et al., 2005; Knowles et al., 2006 and refer to the three references mentioned above).

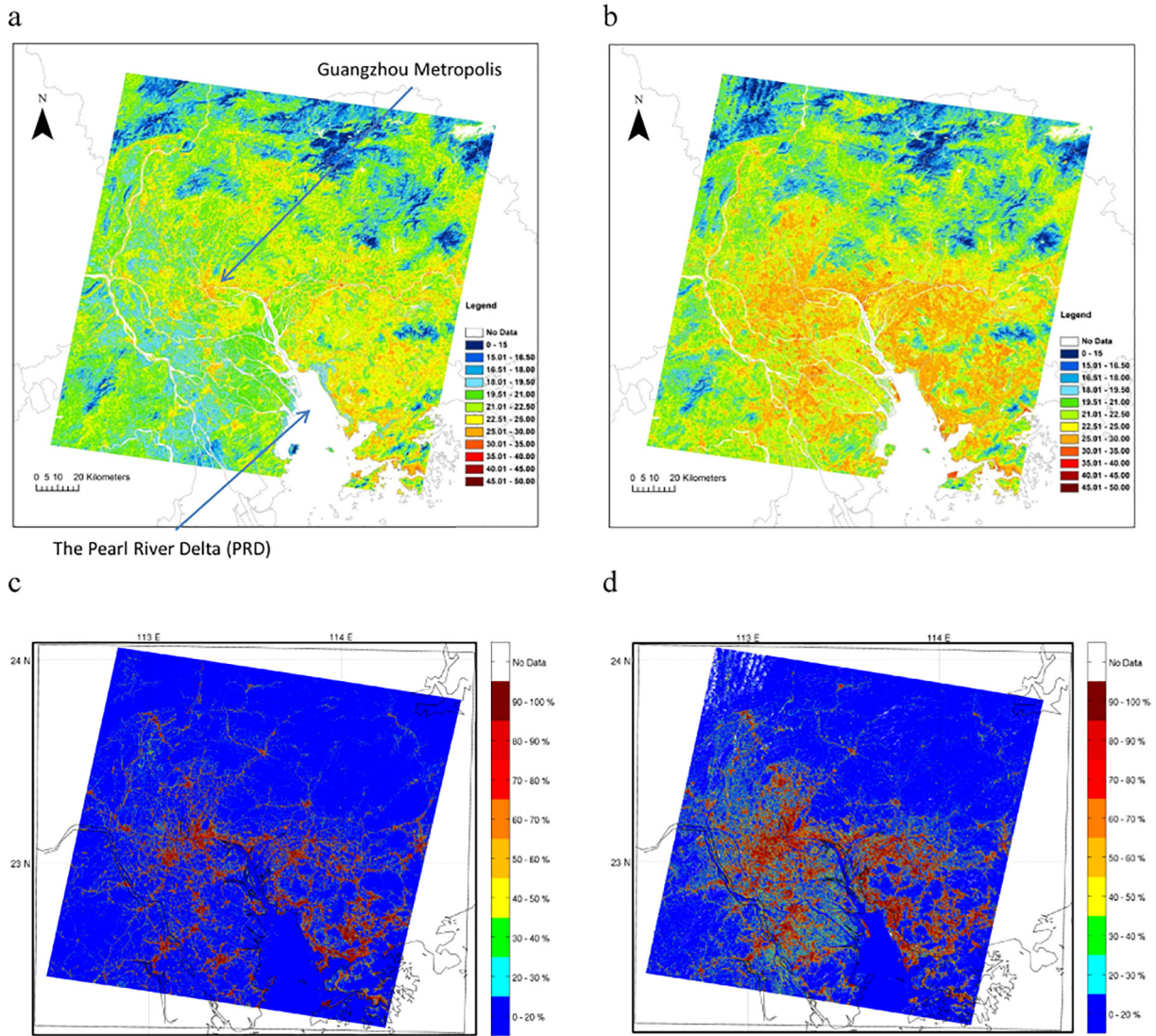


**Fig. 1.** Satellite images over the study area in 1994 and 2010. Land surface temperature ( $^{\circ}\text{C}$ ) distributions observed by the LandSat satellite over the PRD and nearby areas on typical days in fall: (a) 24 October 1994, and (b) 28 October 2010. The post-processed ISA plots on (c) 24 October 1994, and (d) 28 October 2010 are also presented.

#### 2.4. Description of the WRF model and settings of numerical experiments

The WRF model version 3.5.1 coupled with a single-layer urban canopy model (WRF-SLUCM) was used to perform numerical experiments to provide evidence that precipitation was modified by the urbanization effects in the PRD. The coupled model has been used in many urbanization studies (Wang et al., 2009; Tewari et al., 2010; Miao et al., 2011; Chen et al., 2011; Wyszogrodzki et al., 2012). The SLUCM (Kusaka and Kimura, 2004) represents the thermal and dynamic effects of urban areas by taking urban geometry into account in its surface energy budgets and wind shear calculations (Miao and Chen, 2008). The SLUCM was coupled to the Noah land surface model (Chen and Dudhia, 2001), which provided surface sensible and latent heat fluxes and surface skin temperatures as the lower boundary conditions to the WRF model. Other physical parameterizations were used, including the Yonsei University (YSU) planetary boundary layer (PBL) scheme (Noh et al., 2003), the Dudhia shortwave radiation scheme (Dudhia, 1989) and the RRTM longwave radiation scheme (Mlawer et al., 1997). The choice of microphysics and cumulus schemes in the WRF model had substantial impacts on the simulated precipitation in terms of simulated pattern and amount (Wan and Xu, 2011; Liao et al., 2012). In this study, we used the new Kain-Fritsch cumulus scheme (Kain, 2004) and the Lin

et al. (1983) microphysics scheme, which have been reported to give better simulated precipitation results (Liao et al., 2012).

To explore the urbanization effects, precipitation was simulated on 19–20 August 2005 under the influence of the summer monsoon. Initial and boundary conditions for the outermost domain, which covered most of the areas of China, Korea and the northern part of SE Asia, were obtained from the NCEP Operational Global Final (FNL) Analysis dataset with  $1^{\circ} \times 1^{\circ}$  resolution at 6-h intervals. The simulations were made over 3-nesting domains with grid spacings of 27, 9 and 3 km and  $118 \times 112$ ,  $109 \times 91$  and  $91 \times 166$  grid points, respectively. Only the results of the innermost domain are presented here. The innermost domain covered the PRD and the Guangzhou metropolis, similar to the domain shown in Fig. 1 in the work by Wang et al. (2009). There were 31 vertical sigma levels up to 100 hPa and 8 levels below 1 km to better resolve the processes in the PBL. Two sets of simulations, “Pre-urban” and “Urban”, were performed. The former (latter) used the USGS (MODIS) land-use data, with other settings, such as physical parameterizations and initial and boundary conditions, being kept identical. The USGS land-use data were based on the Advanced Very High Resolution Radiometer (AVHRR) data and reflected the distribution of cities such as Guangzhou in 1992. The MODIS land-use data represented the distribution of rapidly urbanized areas in and near the PRD in 2004. The

difference in land-use between the “Pre-urban” and “Urban” simulations is shown in Fig. 1 in the work by Wang et al. (2009). Anthropogenic heat was reported as an important factor to better capture the observed precipitation (Zhong and Yang, 2015) and the spatial variance of surface temperature (Miao et al., 2009) for WRF simulations. Model defaults were used in this study (Zhong and Yang, 2015) for the “Pre-urban” scenario. To represent the likely recent high anthropogenic heat scenario, which is more comparable to that of other megacity studies (Miao et al., 2009; Allen et al., 2011), a maximum value of  $200 \text{ Wm}^{-2}$  (Lin et al., 2008b) was assumed for the “Urban” scenario.

### 3. Results

Fig. 1a and b show the  $T_s$  over the PRD in fall 1994 and 2010 as observed by the Landsat satellite to demonstrate the urbanization effects over the area. The temperature ranged from  $<15^\circ\text{C}$  to  $35^\circ\text{C}$ . Spatial temperature differences between the two years were relatively small at the hilly terrain to the north of the Guangzhou metropolis (i.e., the upper part of Fig. 1a & b); however, much larger differences were observed in the areas over and near the Guangzhou metropolis and the PRD. Compared with natural land uses such as the hilly terrain, urban areas had higher  $T_s$ , as observed by the MODIS satellite over Beijing and New York (Jin et al., 2010). Urbanization is characterized by the increased use of impervious land surfaces, removal of vegetation cover and anthropogenic heat discharge, which explains the higher  $T_s$ . However, it should be noted that the hilly terrain could have had high  $T_s$  but only a small temperature difference between 1994 and 2010. For the Guangzhou metropolis, areas of higher  $T_s$  ( $25\text{--}30^\circ\text{C}$ ) having a radius of  $<8 \text{ km}$  from the city center in 1994 were expanded to a radius of  $20 \text{ km}$  from the center in 2010. Temperature differences of  $5^\circ\text{C}$  between urban and rural areas were evident. The LandSat  $T_s$  data over the study area in 2004 is also provided (Fig. S2), which demonstrates a continuous expansion of urban area over the study period. Fig. 1c and d show the percentage of paved area on the same dates and similar extents of urbanization over and near the Guangzhou metropolis, suggesting a consistent picture to use the surface temperature and ISA to mimic urbanization over the study area. The percentage of paved area given by the ISA plots is an additional valuable information for the urban climate modelling community (e.g. using the WRF-SLUCM) to investigate the climatic effects of land cover evolution.

Fig. 2 shows the variations of ten-year daily precipitation measured at Guangzhou station. Higher precipitation amounts of  $>50 \text{ mm}$  usually occurred in the summer months when the atmosphere was unstable

and had higher moisture content. The M-K test of the long-term precipitation data suggested a positive statistically significant ( $p < 0.05$ ) trend only at the Guangzhou station (Fig. 2, Table 1); no statistically significant trends were found at any other stations. This suggests that long-term increases in city-scale ( $\leq 35 \text{ km}$ ) precipitation existed only at the Guangzhou metropolis, and a regional-scale ( $\geq 100 \text{ km}$ ) increase in precipitation within the study period was not evident. The increase in the ratio of GZ precipitation to total precipitation is highly correlated ( $r = 0.92$ ) to and Urbanization Index in Guangdong (Qin et al., 2012). Plots of annual accumulated precipitation differences between the suburban/rural stations and Guangzhou station also supported increasing precipitation in the Guangzhou metropolis (Fig. 3). The long-term local increase was attributed to the urbanization effects and in turn the UHI effects in the Guangzhou metropolis. The slope for the Guangzhou station dataset, calculated by linear least-squares regression, was  $45.6 \text{ mm}/10 \text{ years}$ . Elsewhere there was an increasing trend of precipitation of  $4.5 \text{ mm}$  per decade over the contiguous United States (Groisman et al., 2005). An increasing trend of  $9.3 \text{ mm}$  per decade in southern Brazil for the 1913–2006 period (Sansigolo and Kayano, 2010) was found. An estimation of the maximum simulated increase rate due to climate change (scenario SRES A2) was  $18.3 \text{ mm}$  per decade over southern China based on Kitoh et al. (2005). The UIEP for our current study was therefore even more significant compared with other studies of precipitation increase available in the literature.

To provide evidence for UIEP over the Guangzhou metropolis, numerical experiments were performed using the WRF-SLUCM model to simulate the typical summer precipitation events on 19–20 August 2005. At that time, the Guangzhou metropolis and PRD were influenced by the summer monsoon, which is associated with a moist maritime air-mass and active convective activities. The selected days had widespread and persistent heavy precipitation due to unstable air, thus the urbanization effects on precipitation could be clearly detected. Precipitation continued until 21 August 2005, when scattered heavy showers were observed, but the unstable weather system was weakened.

Prior to comparing the differences between the “Urban” and “Pre-urban” scenarios, we made a brief comparison of the simulated and observed 24-hour accumulated precipitation at different locations in the study area on 20 August 2005 (Fig. S1). The brief comparison using the observed 24-hour accumulated precipitation provided limited but useful checks on the simulated results in terms of behaviour and pattern. The simulated precipitation was from the “Urban” scenario. Fig. S1 shows that the model skillfully simulated the 24-hour accumulated precipitation amounts measured at 3 stations out of 5; however, the

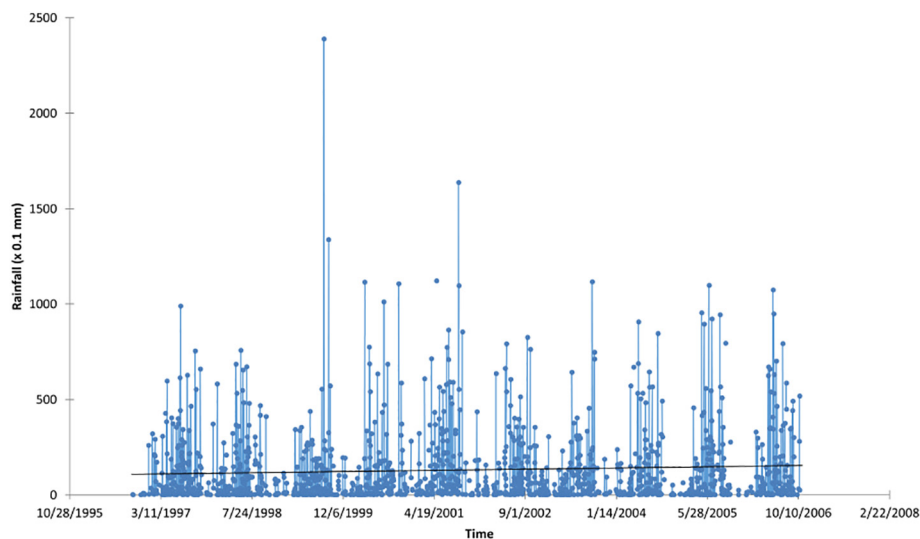


Fig. 2. Long-term record of ground-level measurement of precipitation. The 10-year (1997–2006) daily precipitation ( $\times 0.1 \text{ mm}$ ) measured at Guangzhou station. A trend line is also included.

**Table 1**  
Results of the application of the M-K test.

Station	Z-statistics <sup>a</sup>
GZ	<b>2.41</b>
FG	-1.13
LP	-0.17
NX	-0.81
SG	-0.63

<sup>a</sup> Values significant at the 95% level are in bold.

amounts for the rest were under- or over-predicted. For example, the measured precipitation of 27.4 mm (2.4 mm) at station SG (NX) was close to (well within) the simulated range of 10–25 mm (1–10 mm). The simulated result was also comparable to the measurement at the station FG. A comparison of the precipitation pattern simulated by the model and observed by the surface rain-gauge measurement is shown in Fig. S3. It demonstrates that the model was capable to capture the areas of heavy precipitation (i.e. near 23.0°N, 113.0°E and near 23.0°N, 115.0°E). The differences between the calculated and observed pattern were partially due to relatively few surface stations, such that the data from the few stations might not be enough to resolve all the areas of heavy precipitation. At this point, the model is to be used strictly for numerical experiments to demonstrate the urbanization effects. The intention is not to evaluate the model performance in detail with observations; the challenges for numerical models to simulate precipitation are well-known (e.g., Kain et al., 2008; Wan and Xu, 2011; Liao et al., 2012).

We focus on 20 August 2005 because similar meteorological settings were also featured over the PRD and the Guangzhou metropolis on 19 August 2005. Persistent strong southerly/southwesterly winds associated with the summer monsoon brought moist, unstable air from the South China Sea to the study area. Low-level winds with the aforementioned directions passed over the Guangzhou metropolis and further inland up to 24°N (figure not shown). The heavier precipitation experienced over the area to the north of the Guangzhou metropolis was due to the orographic lifting of moist air (Fig. 4). Fig. 4a shows that the computed 3-hour accumulated precipitation was almost absent

upwind or downwind of the Guangzhou metropolis for the Pre-urban scenario. However, precipitation amounts of up to 20 mm at scattered locations were computed over the metropolis and its immediate downwind areas for the Urban scenario (Fig. 4b). Other smaller urban areas near the PRD also made minor contributions to the precipitation enhancement downwind, i.e., to the northeast of the Guangzhou metropolis. Similar results were also obtained on 19 August 2005, for the Pre-urban scenario, where no apparent precipitation was computed over the Guangzhou metropolis and its immediate downwind areas (Fig. S4). However, up to 12 mm of precipitation was widespread over the metropolis and downwind areas for the Urban scenario. A difference plot (i.e., Urban scenario minus Pre-urban scenario, Fig. S5) for 24-hour accumulated precipitation on 20 August 2005, further supported the UIEP. Therefore, the UIEP over the metropolis and its immediate downwind areas was clearly shown in the numerical experiments. The cause of the precipitation increase was attributed to the strong UHI circulation driven by warmer urban land surfaces. The UHI effects over the Guangzhou metropolis induced a more convective and deeper tropospheric boundary layer, which was reflected in the simulation (Fig. S6). This figure shows that the instantaneous night-time boundary layer height over the Guangzhou metropolis for the Urban scenario was up to 500 m higher than the Pre-urban scenario. However, this value is strictly experimental and is not intended for evaluation of a real situation.

**4. Discussion**

The UIEP has both adverse and beneficial effects on sustainable urban living. The adverse effects include sea-level rise associated with future climate change, which increases flooding potential. An average of 0.5 m sea-level rise by the end of 2100 due to climate change is projected for the southern coast of China (IPCC, 2013). Based on the results mentioned above, UIEP adds a significant burden on coastal defenses because the increasing rate from urbanization is higher compared with that from future climate change. Increases in flooding potential due to higher precipitation amounts pose a significant risk to underground infrastructures as part of sustainable urban development (NAP, 2013). The Guangzhou megacity located in the PRD is ranked in

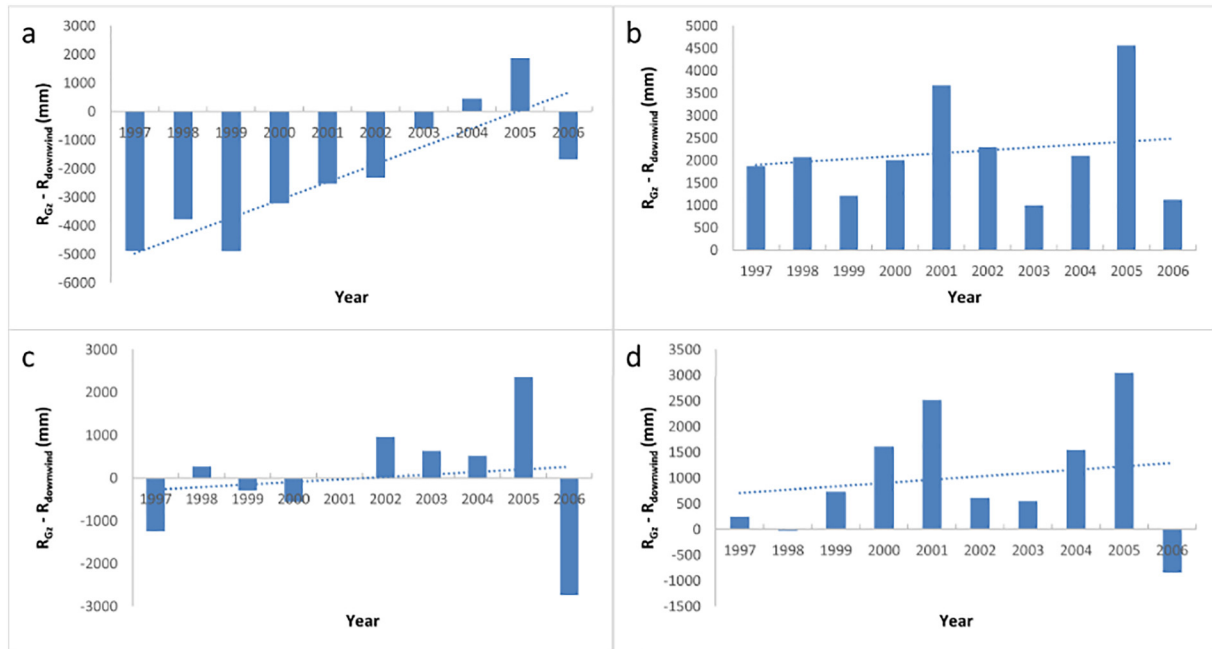


**Fig. 3.** Difference of measured precipitation between stations. Plots of annual accumulated precipitation difference (mm) between (a) Fogang, (b) Naxiong, (c) Lianpin, (d) Shaogua station and Guangzhou station. A trend line is also included. Due to the large range of precipitation differences, the scale of the y-axis for each plot is intended to be different from the others.

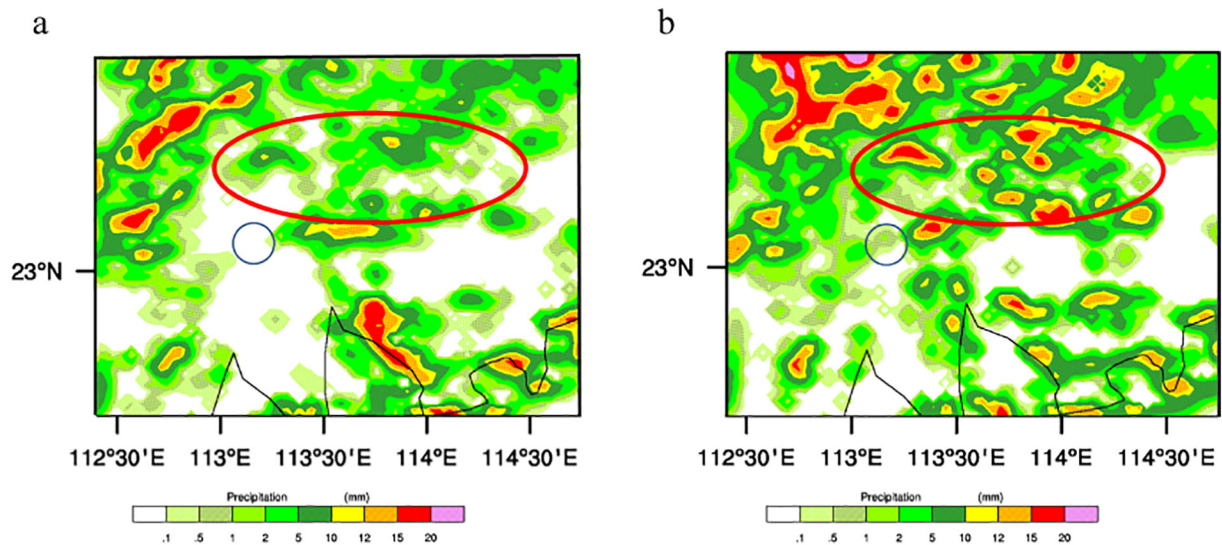


**Fig. 4.** Computed precipitation for the Pre-urban and Urban scenarios. Computed 3-hour night-time accumulated precipitation distribution (mm) over Guangzhou and areas nearby on 20 August 2005, for the (a) Pre-urban and (b) Urban scenarios. The Guangzhou metropolitan (area of influence) is marked by a blue circle (red ellipse). (For interpretation of the references to colour in this figure legend, the reader is referred to the web version of this article.)

the top 20 most vulnerable cities in the world in terms of flooding risk (Ng, 2016 and references therein), because the megacity locates in a low-lying area which is affected by peak river water discharge during wet season and sea water inundation. Therefore, the UIEP effects in Guangzhou should be considered. The findings presented here also have important implications for other rapidly growing large cities worldwide. For example, the pace of urbanization elsewhere in China will continue, especially in the coastal areas of eastern China (Bai et al., 2014). There are many megacities in developing countries located in low-lying areas, river deltas or coastal areas, such as Mumbai and Kolkata in India, Bangkok in Thailand, Jakarta in Indonesia, Dhaka in Bangladesh, Cairo in Egypt and Rio de Janeiro in Brazil. More similar studies are required for these rapidly growing megacities. A correlation between precipitation and mosquito populations (and associated diseases) has been reported. Kruijff (1975) noted that most population studies of adult mosquitoes showed a general relationship between mosquito density and precipitation. Whelan et al. (2003) found five confirmed cases of Murray Valley encephalitis virus infection during high precipitation years compared with one case for other years in Australia. Yamana and Eltahir (2011) used observed precipitation data to drive a mechanistic model to simulate mosquito populations. The findings imply that there might be a direct relationship between precipitation and mosquito-borne diseases; thus, the spread of these diseases, such as the Zika outbreak (see Kutsuna et al. (2014) and articles in the same Issue), due to precipitation increases over cities could be a serious threat to sustainable living.

We also discuss the benefits associated with an increase in precipitation over urban areas. Clearly, this has benefits to cities with water shortages. Urban areas also suffer to some extent from the impacts of UHI (Ng, 2010; Zhou et al., 2016; Lau and Ng, 2013) and heatwaves during summer (Ng, 2014; Wang et al., 2016). The heatwaves cause mortality (e.g., Anderson and Bell, 2011; Chen et al., 2015). A recent study in southern China revealed that an average of 1 °C increase in daily mean temperature above 28.2 °C was associated with a 1.8% increase in mortality (Chan et al., 2012). Prior to the induced precipitation, the associated cloud development reduces the excess heating of the ground surface and in turn the surface air temperature, which results in mitigation of UHI and heatwave effects. However, the weakening of an UHI leads to reduction of the precipitation enhancement over urban areas. With respect to heatwave effects, recent studies have noted the possibility for precipitation to drain energy from the atmosphere and reduce the amount available to generate winds (Pauluis and Dias, 2012). The

weakening of surface winds could exacerbate the heatwave impacts in the urban compacted building environment (Ng et al., 2011). Precipitation changes also affect the estimation of building energy and services via their effects on solar radiation and temperature (Levermore and Parkinson, 2006). A detailed discussion of such complicated feedbacks is beyond the scope of this study; however, the causal relationship of the aforementioned effects is clearly likely to form a new direction in the studies of urban climate and sustainable urban living.

## 5. Conclusions

A precipitation dataset from 1997 to 2006 was analysed for both a rapidly urbanized megacity and nearby suburban/rural stations in southern China. The urbanization effect was evident by the LandSat  $T_s$  product and its post-processed ISA product. Based on the M-K test, a statistically significant increasing trend of precipitation existed only at the megacity station and not at the other stations. This finding indicated that the precipitation increase (45.6 mm per decade) was a city-scale, rather than a regional-scale, phenomenon. The increase was attributed to thermal and dynamical modifications of the tropospheric boundary layer related to urbanization, which was confirmed by the results of our urban WRF-SLUCM (Weather Research & Forecast – Single Layer Urban Canopy Model) simulations. The results also suggested that a long-term regional increase in precipitation, caused by greenhouse gas-induced climate change, for instance, was not evident within the study period. The urbanization-induced increase was found to be higher than the precipitation increase (18.3 mm per decade) expected from future climate change. The direct climate impacts due to rapid urbanization are highlighted with strong implications for urban sustainable development and the planning of effective adaptation strategies. The findings are also relevant to megacities (35 in 2015) in the rest of the world. While the influences of other kind of land use changes (such as water conservancy projects) on our study are small, these changes have to be included for consideration in future studies when appropriate.

Supplementary data to this article can be found online at <http://dx.doi.org/10.1016/j.scitotenv.2017.05.014>.

## Acknowledgments

This study was supported by the Chinese University of Hong Kong (CUHK) VC Discretionary Fund 4930752 and the CUHK Sustainable Development Goals Programme 2016. We acknowledge Mr. WH Liao for

his inputs to our study. The data, model and satellite products used in this study are referenced above in the text.

## References

- Allen, L., Lindberg, F., Grimmond, C.S.B., 2011. Global to city scale urban anthropogenic heat flux: model and variability. *Int. J. Climatol.* 31:1990–2005. <http://dx.doi.org/10.1002/joc.2210>.
- Anderson, G.B., Bell, M.L., 2011. Heat waves in the United States: mortality risk during heat waves and effect modification by heat wave characteristics in 43 U.S. Communities. *Environ. Health Perspect.* 119:210–218. <http://dx.doi.org/10.1289/ehp.1002313>.
- Arnfield, A.J., 2003. Two decades of urban climate research: a review of turbulence, exchanges of energy and water, and the urban heat island. *Int. J. Climatol.* 23:1–26. <http://dx.doi.org/10.1002/joc.859>.
- Bai, X., Shi, P., Liu, Y., 2014. Society: realizing China's urban dream. *Nature* 509:158–160. <http://dx.doi.org/10.1038/509158a>.
- Balling, R.C., Brazel, S.W., 1988. High resolution surface temperature patterns in a complex urban terrain. *Photogramm. Eng. Remote Sens.* 54, 1289–1293.
- Bornstein, R., Lin, Q., 2000. Urban heat islands and summertime convective thunderstorms in Atlanta: three case studies. *Atmos. Environ.* 34:507–516. [http://dx.doi.org/10.1016/S1352-2310\(99\)00374-X](http://dx.doi.org/10.1016/S1352-2310(99)00374-X).
- Brunetti, M., Colacino, M., Maugeri, M., Nanni, T., 2001. Trends in the daily intensity of precipitation in Italy from 1951 to 1996. *Int. J. Climatol.* 21:299–316. <http://dx.doi.org/10.1002/joc.613>.
- Chan, E.Y.Y., Goggins, W.B., Kim, J.J., Griffiths, S.M., 2012. A study of intracity variation of temperature-related mortality and socioeconomic status among the Chinese population in Hong Kong. *J. Epidemiol. Community Health* 66:322–327. <http://dx.doi.org/10.1136/jech.2008.085167>.
- Changnon, S.A., 1979. Rainfall changes in summer caused by St. Louis. *Science* 205:402–404. <http://dx.doi.org/10.1126/science.205.4404.402>.
- Chen, F., Dudhia, J., 2001. Coupling an advanced land surface–hydrology model with the Penn State–NCAR MM5 Modeling System. Part I: model implementation and sensitivity. *Mon. Weather Rev.* 129:569–585. [http://dx.doi.org/10.1175/1520-0493\(2001\)129<0569:caalsh>2.0.co;2](http://dx.doi.org/10.1175/1520-0493(2001)129<0569:caalsh>2.0.co;2).
- Chen, X.-L., Zhao, H.-M., Li, P.-X., Yin, Z.-Y., 2006. Remote sensing image-based analysis of the relationship between urban heat island and land use/cover changes. *Remote Sens. Environ.* 104:133–146. <http://dx.doi.org/10.1016/j.rse.2005.11.016>.
- Chen, F., Kusaka, H., Bornstein, R., Ching, J., Grimmond, C.S.B., Grossman-Clarke, S., Loridan, T., Manning, K.W., Martilli, A., Miao, S., Sailor, D., Salamanca, F.P., Taha, H., Tewari, M., Wang, X., Wyszogrodzki, A.A., Zhang, C., 2011. The integrated WRF/urban modelling system: development, evaluation, and applications to urban environmental problems. *Int. J. Climatol.* 31:273–288. <http://dx.doi.org/10.1002/joc.2158>.
- Chen, K., Huang, L., Zhou, L., Ma, Z., Bi, J., Li, T., 2015. Spatial analysis of the effect of the 2010 heat wave on stroke mortality in Nanjing, China. *Sci. Rep.* 5:10816. <http://dx.doi.org/10.1038/srep10816>.
- Dixon, P.G., Mote, T.L., 2003. Patterns and causes of Atlanta's urban Heat Island-initiated precipitation. *J. Appl. Meteorol.* 42:1273–1284. [http://dx.doi.org/10.1175/1520-0450\(2003\)042<1273:pacoau>2.0.co;2](http://dx.doi.org/10.1175/1520-0450(2003)042<1273:pacoau>2.0.co;2).
- Dousset, B., Gourmelon, F., 2003. Satellite multi-sensor data analysis of urban surface temperatures and landcover. *ISPRS J. Photogramm. Remote Sens.* 58:43–54. [http://dx.doi.org/10.1016/S0924-2716\(03\)00016-9](http://dx.doi.org/10.1016/S0924-2716(03)00016-9).
- Dudhia, J., 1989. Numerical study of convection observed during the winter monsoon experiment using a mesoscale two-dimensional model. *J. Atmos. Sci.* 46:3077–3107. [http://dx.doi.org/10.1175/1520-0469\(1989\)046<3077:nsocod>2.0.co;2](http://dx.doi.org/10.1175/1520-0469(1989)046<3077:nsocod>2.0.co;2).
- Gilbert, R.O., 1987. *Statistical Methods for Environmental Pollution Monitoring*. Van Nostrand Reinhold Co., New York.
- van Ginkel, H., 2008. Urban future. *Nature* 456:32–33. <http://dx.doi.org/10.1038/twas08.32a>.
- Groisman, P.Y., Knight, R.W., Easterling, D.R., Karl, T.R., Hegerl, G.C., Razuvaev, V.N., 2005. Trends in intense precipitation in the climate record. *J. Clim.* 18:1326–1350. <http://dx.doi.org/10.1175/JCLI3339.1>.
- Hjelmfelt, M.R., 1982. Numerical simulation of the effects of St. Louis on mesoscale boundary-layer airflow and vertical air motion: simulations of urban vs non-urban effects. *J. Appl. Meteorol.* 21:1239–1257. [http://dx.doi.org/10.1175/1520-0450\(1982\)021<1239:nsoteo>2.0.co;2](http://dx.doi.org/10.1175/1520-0450(1982)021<1239:nsoteo>2.0.co;2).
- Huang, C., Zhang, M., Zou, J., Zhu, A.-X., Chen, X., Mi, Y., Wang, Y., Yang, H., Li, Y., 2015. Changes in land use, climate and the environment during a period of rapid economic development in Jiangsu Province, China. *Sci. Total Environ.* 536:173–181. <http://dx.doi.org/10.1016/j.scitotenv.2015.07.014>.
- IPCC, 2007. *Climate Change 2007: Working Group I: The Physical Science Basis*. Cambridge University Press, New York.
- IPCC, 2013. *Climate Change 2013: Working Group I: The Physical Science Basis*. Cambridge University Press, New York.
- Jin, M., Shepherd, J.M., Zheng, W., 2010. Urban surface temperature reduction via the urban aerosol direct effect: a remote sensing and WRF model sensitivity study. *Adv. Meteorol.* 2010:1–14. <http://dx.doi.org/10.1155/2010/681587>.
- Joshi, M.K., Pandey, A.C., 2011. Trend and spectral analysis of rainfall over India during 1901–2000. *J. Geophys. Res.* 116. <http://dx.doi.org/10.1029/2010jd014966>.
- Kain, J.S., 2004. The Kain–Fritsch convective parameterization: an update. *J. Appl. Meteorol.* 43:170–181. [http://dx.doi.org/10.1175/1520-0450\(2004\)043<0170:tkcpau>2.0.co;2](http://dx.doi.org/10.1175/1520-0450(2004)043<0170:tkcpau>2.0.co;2).
- Kain, J.S., Weiss, S.J., Dembek, S.R., Levit, J.J., Bright, D.R., Case, J.L., Schwartz, C.S., 2008. Severe-weather forecast guidance from the first generation of large domain convection-allowing models: Challenges and opportunities. This Paper Was Presented at 24th Conference on Severe Local Storms. *Am. Meteorol. Soc. Savannah USA*.
- Kitoh, A., Hosaka, M., Adachi, Y., Kamiguchi, K., 2005. Future projections of precipitation characteristics in East Asia simulated by the MRI CGCM2. *Adv. Atmos. Sci.* 22: 467–478. <http://dx.doi.org/10.1007/bf02918481>.
- Knowles, N., Dettinger, M.D., Cayan, D.R., 2006. Trends in snowfall versus rainfall in the Western United States. *J. Clim.* 19:4545–4559. <http://dx.doi.org/10.1175/JCLI3850.1>.
- Krujif, H.A.M.D., 1975. The relation between rainfall and mosquito populations. *Trop. Ecol. Syst.* 11:61–65. [http://dx.doi.org/10.1007/978-3-642-88533-4\\_6](http://dx.doi.org/10.1007/978-3-642-88533-4_6).
- Kusaka, H., Kimura, F., 2004. Thermal effects of urban canyon structure on the nocturnal Heat Island: numerical experiment using a mesoscale model coupled with an urban canopy model. *J. Appl. Meteorol.* 43:1899–1910. <http://dx.doi.org/10.1175/jam2169.1>.
- Kutsuna, S., Kato, Y., Takasaki, T., Moi, M., Kotaki, A., Uemura, H., Matono, T., Fujiya, Y., Mawatari, M., Takeshita, N., Hayakawa, K., Kanagawa, S., Ohmagari, N., 2014. Two cases of Zika fever imported from French Polynesia to Japan, December to January 2013. *Euro Surveill.* 19:20683. <http://dx.doi.org/10.2807/1560-7917.es2014.19.4.20683>.
- Lau, K.L., Ng, E., 2013. An investigation of urbanization effect on urban and rural Hong Kong using a 40-year extended temperature record. *Lands. Urban Plan.* 114:42–52. <http://dx.doi.org/10.1016/j.landurbplan.2013.03.002>.
- Levermore, G.J., Parkinson, J.B., 2006. Analyses and algorithms for new test reference years and design summer years for the UK. *Build. Serv. Eng. Res. Technol.* 27: 311–325. <http://dx.doi.org/10.1177/014362440601037>.
- Liao, J.B., Wang, X.M., Xia, B.C., Wang, T.J., Wang, Z.M., 2012. The effects of different physics and cumulus parameterization schemes in WRF on heavy rainfall simulation in PRD. *J. Trop. Meteorol.* 28, 461–470.
- Liebmann, B., Vera, C.S., Carvalho, L.M.V., Camilloni, I.A., Hoerling, M.P., Allured, D., Barros, V.R., Báez, J., Bidegain, M., 2004. An observed trend in Central South American precipitation. *J. Clim.* 17:4357–4367. <http://dx.doi.org/10.1175/3205.1>.
- Lin, Y.L., Farley, R.D., Orville, H.D., 1983. Bulk parameterization of the snow field in a cloud model. *J. Clim. Appl. Meteorol.* 22:1065–1092. [http://dx.doi.org/10.1175/1520-0450\(1983\)022<1065:bptsf>2.0.co;2](http://dx.doi.org/10.1175/1520-0450(1983)022<1065:bptsf>2.0.co;2).
- Lin, C.Y., Chen, W., Liu, S., Liou, Y., Liu, G., Lin, T., 2008a. Numerical study of the impact of urbanization on the precipitation over Taiwan. *Atmos. Environ.* 42:2934–2947. <http://dx.doi.org/10.1016/j.atmosenv.2007.12.054>.
- Lin, C.Y., Chen, F., Huang, J., Chen, W.C., Liou, Y.A., Chen, W.N., Liu, S.C., 2008b. Urban heat island effect and its impact on boundary layer development and land–sea circulation over northern Taiwan. *Atmos. Environ.* 42:5635–5649. <http://dx.doi.org/10.1016/j.atmosenv.2008.03.015>.
- Miao, S., Chen, F., 2008. Formation of horizontal convective rolls in urban areas. *Atmos. Res.* 89:298–304. <http://dx.doi.org/10.1016/j.atmosres.2008.02.013>.
- Miao, S., Chen, F., Lemone, M.A., Tewari, M., Li, Q., Wang, Y., 2009. An observational and modeling study of characteristics of urban Heat Island and boundary layer structures in Beijing. *J. Appl. Meteorol. Climatol.* 48:484–501. <http://dx.doi.org/10.1175/2008jamc1909.1>.
- Miao, S., Chen, F., Li, Q., Fan, S., 2011. Impacts of urban processes and urbanization on summer precipitation: a case study of heavy rainfall in Beijing on 1 August 2006. *J. Appl. Meteorol. Climatol.* 50:806–825. <http://dx.doi.org/10.1175/2010jamc2513.1>.
- Mlawer, E.J., Taubman, S.J., Brown, P.D., Iacono, M.J., Clough, S.A., 1997. Radiative transfer for inhomogeneous atmospheres: RRTM, a validated correlated-k model for the longwave. *J. Geophys. Res. Atmos.* 102:16663–16682. <http://dx.doi.org/10.1029/97jd00237>.
- Naccarato, K.P., Pinto, O., Pinto, I.R.C.A., 2003. Evidence of thermal and aerosol effects on the cloud-to-ground lightning density and polarity over large urban areas of south-eastern Brazil. *Geophys. Res. Lett.* 30. <http://dx.doi.org/10.1029/2003gl017496>.
- NAP, 2013. *Underground Engineering for Sustainable Urban Development*. National Research Council <https://www.nap.edu/catalog/14670/underground-engineering-for-sustainable-urban-development> (Accessed 17.03.03).
- Ng, E., 2010. *Designing High-density Cities for Social and Environmental Sustainability*. Earthscan, New York.
- Ng, E., 2014. Editorial: mitigation climate change - a research imperative. *Archit. Sci. Rev.* 57:1–3. <http://dx.doi.org/10.1080/00038628.2014.901655>.
- Ng, E., 2016. Adapting Asian cities to climate and urban climatic changes: a Chinese tale. *Urban Climate News* (59). <http://urban-climate.org/newsletters/IAUC059.pdf> (Accessed 17.03.03).
- Ng, E., Yuan, C., Chen, L., Ren, C., Fung, J.C., 2011. Improving the wind environment in high-density cities by understanding urban morphology and surface roughness: a study in Hong Kong. *Lands. Urban Plan.* 101:59–74. <http://dx.doi.org/10.1016/j.landurbplan.2011.01.004>.
- Nichol, J., 2009. An emissivity modulation method for spatial enhancement of thermal satellite images in urban Heat Island analysis. *Photogramm. Eng. Remote Sens.* 75: 547–556. <http://dx.doi.org/10.14358/pers.75.5.547>.
- Nichol, J.E., Fung, W.Y., Lam, K.-S., Wong, M.S., 2009. Urban heat island diagnosis using ASTER satellite images and 'in situ' air temperature. *Atmos. Res.* 94:276–284. <http://dx.doi.org/10.1016/j.atmosres.2009.06.011>.
- Noh, Y., Cheon, W.G., Hong, S.Y., Raasch, S., 2003. Improvement of the K-profile model for the planetary boundary layer based on large eddy simulation data. *Bound.-Layer Meteorol.* 107:401–427. <http://dx.doi.org/10.1023/A:1022146015946>.
- Pauluis, O., Dias, J., 2012. Satellite estimates of precipitation-induced dissipation in the atmosphere. *Science* 335:953–956. <http://dx.doi.org/10.1126/science.1215869>.
- Pielke, R.A., Adegoke, J., Beltrán-Przekurat, A., Hiemstra, C.A., Lin, J., Nair, U.S., Niyogi, D., Nobis, T.E., 2007. An overview of regional land-use and land-cover impacts on rainfall. *Tellus B* 59. <http://dx.doi.org/10.3402/tellusb.v59i3.17038>.
- Project METROMEX, 1974. *Bull. Am. Meteorol. Soc.* 55:86–121. [http://dx.doi.org/10.1175/1520-0477\(1974\)055<0086:pm>2.0.co;2](http://dx.doi.org/10.1175/1520-0477(1974)055<0086:pm>2.0.co;2).
- Qin, Z., Zhang, J., Luo, S., Zhang, J., Li, Y., 2012. Study on coordinative development between urbanization and eco-environment in Guangdong Province. *Ecol. Sci.* 31, 42–47 (in Chinese).
- Quah, A.K., Roth, M., 2012. Diurnal and weekly variation of anthropogenic heat emissions in a tropical city, Singapore. *Atmos. Environ.* 46:92–103. <http://dx.doi.org/10.1016/j.atmosenv.2011.10.015>.
- Sansigolo, C.C.B.A., Kayano, M.T., 2010. Trends of seasonal maximum and minimum temperatures and precipitation in southern Brazil for the 1913–2006 period. *Theor. Appl. Climatol.* 101:209–216. <http://dx.doi.org/10.1007/s00704-010-0270-2>.
- Sawaya, K., 2003. Extending satellite remote sensing to local scales: land and water resource monitoring using high-resolution imagery. *Remote Sens. Environ.* 88: 144–156. <http://dx.doi.org/10.1016/j.rse.2003.04.0006>.
- Tewari, M., Kusaka, H., Chen, F., Coirier, W.J., Kim, S., Wyszogrodzki, A.A., Warner, T.T., 2010. Impact of coupling a microscale computational fluid dynamics model with a

- mesoscale model on urban scale contaminant transport and dispersion. *Atmos. Res.* 96:656–664. <http://dx.doi.org/10.1016/j.atmosres.2010.01.006>.
- United Nations, Department of Economic and Social Affairs, Population Division, 2015. *World Urbanization Prospects: The 2014 Revision*. United Nations, New York.
- Wan, Q., Xu, J., 2011. A numerical study of the rainstorm characteristics of the June 2005 flash flood with WRF/GSI data assimilation system over south-east China. *Hydrol. Process.* 25:1327–1341. <http://dx.doi.org/10.1002/hyp.7882>.
- Wang, X., Chen, F., Wu, Z., Zhang, M., Tewari, M., Guenther, A., Wiedinmyer, C., 2009. Impacts of weather conditions modified by urban expansion on surface ozone: comparison between the Pearl River Delta and Yangtze River Delta regions. *Adv. Atmos. Sci.* 26:962–972. <http://dx.doi.org/10.1007/s00376-009-8001-2>.
- Wang, W., Zhou, W., Li, X., Wang, X., Wang, D., 2016. Synoptic-scale characteristics and atmospheric controls of summer heat waves in China. *Clim. Dyn.* 46:2923–2941. <http://dx.doi.org/10.1007/s00382-015-2741-8>.
- Whelan, P.L., Jacups, S.P., Melville, L., Broom, A., Currie, B.J., Krause, V.L., Porigneaux, P., 2003. Rainfall and vector mosquito numbers as risk indicators for mosquito-borne disease in Central Australia. *Commun. Dis. Intell.* 27, 110–116.
- Wu, C., Murray, A.T., 2003. Estimating impervious surface distribution by spectral mixture analysis. *Remote Sens. Environ.* 84:493–505. [http://dx.doi.org/10.1016/s0034-4257\(02\)00136-0](http://dx.doi.org/10.1016/s0034-4257(02)00136-0).
- Wyszogrodzki, A.A., Miao, S., Chen, F., 2012. Evaluation of the coupling between mesoscale-WRF and LES-EULAG models for simulating fine-scale urban dispersion. *Atmos. Res.* 118:324–345. <http://dx.doi.org/10.1016/j.atmosres.2012.07.023>.
- Yamana, T.K., Eltahir, E.A.B., 2011. On the use of satellite-based estimates of rainfall temporal distribution to simulate the potential for malaria transmission in rural Africa. *Water Resour. Res.* 47. <http://dx.doi.org/10.1029/2010wr009744>.
- Zhang, N., Gao, Z., Wang, X., Chen, Y., 2010. Modeling the impact of urbanization on the local and regional climate in Yangtze River Delta, China. *Theor. Appl. Climatol.* 102: 331–342. <http://dx.doi.org/10.1007/s00704-010-0263-1>.
- Zhong, S., Yang, X.-Q., 2015. Mechanism of urbanization impact on a summer cold-frontal rainfall process in the greater Beijing metropolitan area. *J. Appl. Meteorol. Climatol.* 54:1234–1247. <http://dx.doi.org/10.1175/jamc-d-14-0264.1>.
- Zhou, D., Zhang, L., Hao, L., Sun, G., Liu, Y., Zhu, C., 2016. Spatiotemporal trends of urban heat island effect along the urban development intensity gradient in China. *Sci. Total Environ.* 544:617–626. <http://dx.doi.org/10.1016/j.scitotenv.2015.11.168>.
- Ziv, B., Saaroni, H., Pargament, R., Harpaz, T., Alpert, P., 2013. Trends in rainfall regime over Israel, 1975–2010, and their relationship to large-scale variability. *Reg. Environ. Chang.* 14:1751–1764. <http://dx.doi.org/10.1007/s10113-013-0414-x>.